Supporting Information

Haessler et al. 10.1073/pnas.1014920108

SI Text

SI Materials and Methods. ***Flow cytometry.*** Cells were fixed, permeabilized with Cytofix/Cytoperm (BD Biosciences, Allschwil, Switzerland), and subsequently blocked with hybridoma supernatant containing 24G.2 for 1 hr. Cells were stained with PB or AF-647 conjugated antibodies against MHCII (FITC), CD86 (PE), CCR7 (PE-Cy7) and CD11c (all from eBioscience, Frankfurt, Germany), scanned on a CyAnADP (Dako Cytomation, Glostrup, Denmark), and analyzed with Flowjo software (Tree Star, Ashland, OR).

ELISA to quantify DC-secreted CCL19. 10^6 cells/mL were cultured for 18 h in triplicate in 2D or 3D conditions, respectively. For 2D conditions, 100 μL of supernatant was used for each assay, while for 3D conditions, the matrix was digested with Collagenase D (Roche, Basel, Switzerland) for 30 min. at 37 °C and 100 μL of the digested gel was used for quantification. The ELISA was performed according to manufacturer's instructions for mCCL19 DuoSet ELISAs (R and D Systems).

Chemokine-matrix ECM binding properties. A modified ELISA assay was used to determine the binding properties for CCL21 and CCL19 to the extracellular matrix (ECM) used in these experiments. 1.5 mg/mL collagen with 10% Matrigel (MG) was prepared, diluted 1:100 in PBS, added to the wells (100 μL/well) of a 96 well plate (Maxisorp, Thermo Scientific, Langenselbold, Germany), and incubated overnight. After blocking with 2.5% Casein for 2 h, increasing concentrations of CCL21 and CCL19 solution were added and incubated for 2 h. Bound concentrations of CCL21 and CCL19 were quantified with DuoSet ELISA kits according manufacturer's instructions. Data were analyzed and K_D determined with Prism (GraphPad Software, La Jolla, CA) using the algorithm for "one-site total binding;" in other words by fitting the data to the following equation:

$$\mathrm{Abs} = B_{\max}\frac{C_i}{K_D + C_i} + \mathrm{NS}(C_i). \qquad \textbf{[S1]}$$

Where Abs = Optical absorbance (after background is subtracted), B_{Max} = maximum specific binding (in units of absorbance), C_i = concentration of ligandadded, and NS = slope of nonspecific binding.

Theoretical model for dependence of chemotactic sensitivity on chemokine concentration gradient. We hypothesize that the cell chemotactic sensitivity (expressed as the average cell velocity along the direction of chemokine gradient) is proportional to the difference of the fractional ligand receptor occupancy at the front vs back of the cell. In our experiments, cells are exposed to a linear chemokine (CCL19 or CCL21, both ligand to CCR7) gradient along x direction. At equilibrium state, the fractional ligand receptor occupancy is $\frac{C}{C+K_D}$, where C is the chemokine concentration, and K_D is the association constant of CCR7 to its ligand CCL19 or CCL21. The difference of the fractional ligand occupancy at the front and back of the cell is $(\frac{C}{C+K_D})_{\mathrm{front}} - (\frac{C}{C+K_D})_{\mathrm{back}}$. Because the cell is polarized along the direction of the gradient, and the length of the cell is small comparing to the width of the channel, this difference can be calculated as : $(\frac{C}{C+K_D})|_{x=x+l} - (\frac{C}{C+K_D})|_{x=x} = \frac{lK_D\nabla C}{(C+K_D)^2} \cong \frac{lK_D\nabla C}{(C_{\mathrm{avg}}+K_D)^2} = A\frac{\nabla C}{(C_{\mathrm{avg}}+K_D)^2}$.

Here C_{avg} is the average chemokine concentration at the center of the channel, and l is the length of the cell, and A is a constant.

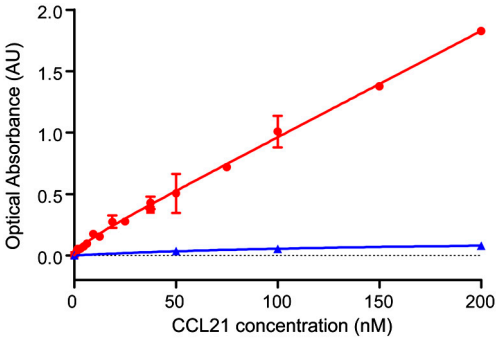

Fig. S1. Binding affinity of CCL21/CCL19 to the extracellular matrix. Experimental data (symbols) and computational fits to Eq. **S1** (solid lines) to estimate K_D for CCL19 (blue) and CCL21 (red) to the 1.5 mg/mL collagen—10% MG matrix. Resulting K_D values were 7 nM (±8 nM) for CCL21 and 160 nM (±20 nM) for CCL19.

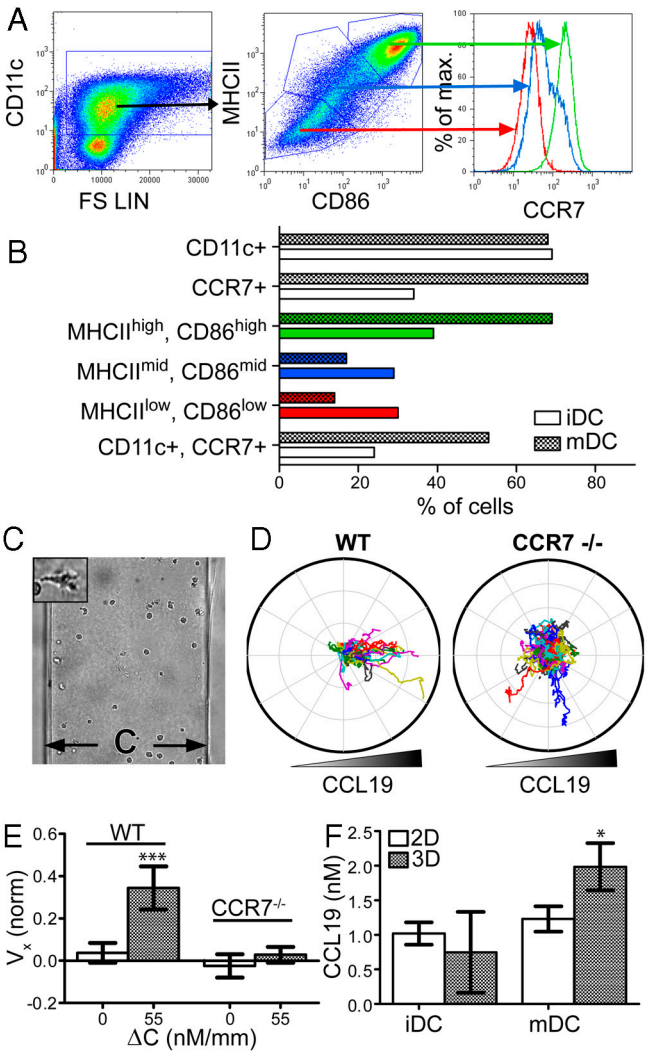

Fig. S2. Murine bone marrow derived dendritic cells show a typical mature phenotype after LPS maturation and respond to CCL19 in a CCR7-dependant manner. (*A*–*B*) Molecular profiling of immature and LPS-matured dendritic cells (iDCs and mDCs, respectively) using flow cytometry. (*A*) Gating for (*i*) $CD86^{low}$ $MHCII^{low}$ cells, green; (*ii*) $CD86^{mid}$ $MHCII^{mid}$ cells, blue; and (*iii*) $CD86^{high}$ $MHCII^{high}$ cells, red. (*B*) Percent iDCs and mDCs positive for CD11c, MHCII, CD86, and CCR7; colors represent the indicated gates in *A*. (*C*–*E*) Functionality of CCR7 for DC chemotaxis in 3D. (*C*) Brightfield image of mDCs inside the center channel with channel borders (black arrows); width = 900 mm. Inset shows a single migrating DC. (*D*) Trajectories of wild type and $CCR7^{-/-}$ DCs in a CCL19 gradient of 55 nM/mm. (*E*) Net chemotactic migration velocity of wild type and $CCR7^{-/-}$ DCs towards CCL19 gradients of 0 and 55 nM/mm. (*F*) Secretion of CCL19 by iDCs and mDCs in 2D vs. 3D conditions after 24 h.

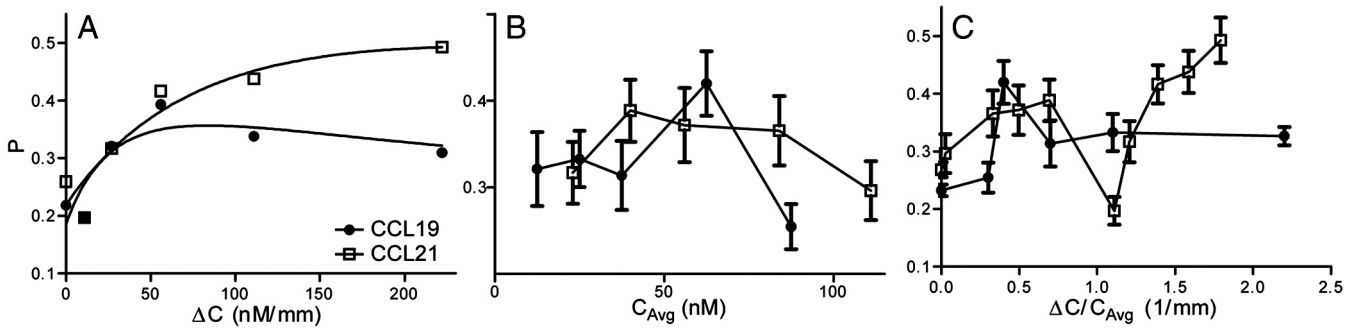

Fig. S3. Migratory persistence in response to CCR7 ligand gradients mirrors directed migration. *P* is defined as the ratio of net distance travelled over the total distance travelled, regardless of direction. (*A*) *P* as a function of concentration difference (∇C) with fixed. $\nabla C/C_{Avg}$ Solid lines show the data fits to Eq. **S1**, yielding K_D values of 80 nM (±30 nM) for CCL19 and 260 nM (±190 nM). (*B*) *P* as a function of average concentration C_{Avg}, with ∇C held constant at 28 nM/mm. (*C*) *P* as a function of % gradient ($\nabla C/C_{Avg}$). All data represent $n \geq 2$, each averaging 70–850 data points.